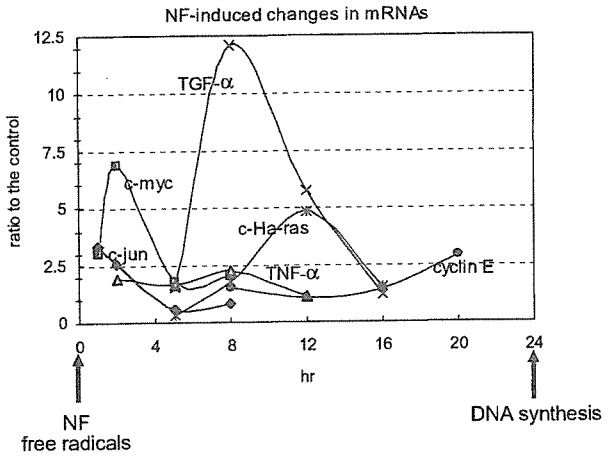

Fig. 2. Changes in the mRNAs of genes induced by NF. Free radicals produced during NF metabolism may lead to immediate early genes such as c-jun, c-myc, and possibly TNF-α. This results in the priming of hepatocytes which have now acquired competence for cell growth. These events are followed by proliferative stimulation by TNF-α, or TGF-α, or both. The expression of c-Ha-ras, in concert with other genes, including cyclin E, may conceivably allow hepatocytes to pass through the restriction point and enter the S phase of the cell cycle, finally culminating in DNA synthesis.

be seen whether the inhibition of the above genes is an indirect result of free radical scavenging, eliminating the trigger itself and interrupting the cascade at the root, or a direct inhibitory effect on each step of the cascade by NAC, or even both, although the former is more likely considering the two-fold antioxidant action of NAC.

It is intriguing that a substantial portion of the changes associated with proliferation is shared among diverse, chemically unrelated substances acting as mitogens. Although the relative importance of each gene is yet to be elucidated, further studies, including changes at the protein level and activation of various transcription factors, should contribute to a better understanding of the process.

Acknowledgments

The authors would like to express deep gratitude to Kazuhiko Suzuki, Ryoichi Ohtsuka, and Makio Takeda for their valuable advice and suggestions, as well as Satoru Sasaki and Kenji Nakano for their technical assistance and support. Their help has been indispensable throughout the course of this study.

References

Chanda S, Mangipudy RS, Warbritton A, et al. Stimulated hepatic tissue repair underlies heteroprotection by thioacetamide against acetaminophen-induced lethality. Hepatology 1995;21:477–86.

Columbano A, Shinozuka H. Liver regeneration versus direct hyperplasia. FASEB J 1996;10:1118–28.

Columbano A, Ledda GM, Sirigu P, et al. Liver cell proliferation induced by a single dose of lead nitrate. Am J Pathol 1983;110:83–8.

Coni P, Pichiri-Coni G, Ledda-Columbano GM, et al. Liver hyperplasia is not necessarily associated with increased expression of c-fos and c-myc mRNA. Carcinogenesis 1990; 11:835–9.

Coni P, Simbula G, De Prati AC, et al. Differences in the steady-state levels of c-fos, c-jun and c-myc messenger RNA during mitogen-induced liver growth and compensatory regeneration. Hepatology 1993;17:1109–16.

Connell-Crowley L, Elledge SJ, Harper JW. G1 cyclin-dependent kinases are sufficient to initiate DNA synthesis in quiescent human fibroblasts. Curr Biol 1998; 8:65–8.

Fausto N. Hepatic regeneration. Zakim D, Boyer T, editors. Hepatology. A textbook of liver disease, Vol. 1. Pennsylvania: W.B. Saunders Company; 1996. p. 32–58.

Fausto N, Mead JE. Biology of disease. Regulation of liver growth: protooncogenes and transforming growth factors. Lab Invest 1989;60:4–13.

Fausto N, Laird AD, Webber EM. Role of growth factors and cytokines in hepatic regeneration. FASEB J 1995;9: 1527–36.

Gallucci RM, Simeonova PP, Toriumi W, et al. TNF-α regulates transforming growth factor-α expression in regenerating murine liver and isolated hepatocytes. J Immunol 2000;164:872–8.

Goldsworthy TL, Goldsworthy SM, Sprankle CS, et al. Expression of myc, fos and Ha-ras associated with chemically induced cell proliferation in the rat liver. Cell Prolif 1994;27:269–78.

Hagenäs L, Plöen L, Ritzen EM. The effect of nitrofurazone on the endocrine, secretory and spermatogenic functions of the rat testis. Andrologia 1978;10:107–26.

Iatropoulos MJ, Williams GM. Proliferation markers. Exp Toxicol Pathol 1996;48:175–81.

Ito K, Ishida K, Takeuchi A, et al. Nitrofurazone induces non-regenerative hepatocyte proliferation in rats. Exp Toxicol Pathol 2002;53:421–6.

Ito K, Kajikawa S, Nii A, et al. Antioxidants suppress nitrofurazone-induced proliferation of hepatocytes. Exp Toxicol Pathol 2003;55:247–50.

Ito K, Takeuchi A, Nii A, et al. Nitrofurazone at a high dose induces hepatocyte and adrenal necrosis in rats. J Toxicol Pathol 2004;17:59–61.

Kari FW, Huff JE, Leininger J, et al. Toxicity and carcinogenicity of nitrofurazone in F344/N rats and B6C3F1 mice. Food Chem Toxicol 1989;27:129–37.

Ledda-Columbano GM, Coni P, Simbula G, et al. Compensatory regeneration, mitogen-induced liver growth, and multistage chemical carcinogenesis. Environ Health Perspect 1993;101(Suppl. 5):163–8.

Mangipudy RS, Chanda S, Mehendale HM. Hepatocellular regeneration: key to thioacetamide autoprotection. Pharmacol Toxicol 1995a;77:182–8.

Mangipudy RS, Chanda S, Mehendale HM. Tissue repair response as a function of dose in thioacetamide hepatotoxicity. Environ Health Perspect 1995b;103:260–7.

Masuhara M, Ogasawara H, Katyal SL, et al. Cyclosporine stimulates hepatocyte proliferation and accelerates development of hepatocellular carcinomas in rats. Carcinogenesis 1993;14:1579–84.

Nachtomi E, Farber E. Ethylene dibromide as a mitogen for liver. Lab Invest 1978;38:279–83.

Peterson FJ, Mason RP, Hovsepian J, et al. Oxygen-sensitive and -insensitive nitroreduction by *Escherichia coli* and rat hepatic microsomes. J Biol Chem 1979;254:4009–14.

Rao PS, Mangipudy RS, Mehendale HM. Tissue injury and repair as parallel and opposing responses to CCl_4 hepatotoxicity: a novel dose-response. Toxicology 1997;118:181–93.

Remacle J, Raes M, Toussaint O, et al. Low levels of reactive oxygen species as modulators of cell function. Mutat Res 1995;316:103–22.

Roberts JM. Evolving ideas about cyclins. Cell 1999;98:129–32.

Roberts RA, Soames AR, Gill JH, et al. Non-genotoxic hepatocarcinogens stimulate DNA synthesis and their withdrawal induces apoptosis, but in different hepatocyte populations. Carcinogenesis 1995;16:1693–8.

Rusyn I, Yamashina S, Segal BH, et al. Oxidants from nicotinamide adenine dinucleotide phosphate oxidase are involved in triggering cell proliferation in the liver due to peroxisome proliferators. Cancer Res 2000;60:4798–803.

Sherr CJ, Roberts JM. CDK inhibitors: positive and negative regulators of G1-phase progression. Genes Dev 1999;13:1501–12.

Shinozuka H, Kubo Y, Katyal L, et al. Roles of growth factors and of tumor necrosis factor-alpha on liver cell proliferation induced in rats by lead nitrate. Lab Invest 1994;71:35–41.

Soni MG, Mehendale HM. Role of tissue repair in toxicologic interactions among hepatotoxic organics. Environ Health Perspect 1998;106(Suppl. 6):1307–17.

Takuwa N, Takuwa Y. Ras activity late in G1 phase required for $p27^{kip1}$ downregulation, passage through the restriction point, and entry into S phase in growth factor-stimulated NIH 3T3 fibroblasts. Mol Cell Biol 1997;17:5348–58.

Tatsumi K, Kitamura S, Yoshimura H, et al. Reduction of nitrofuran derivatives by xanthine oxidase and microsomes. Arch Biochem Biophys 1976;175:131–7.

Tomiya T, Ogata I, Fujiwara K. Transforming growth factor α levels in liver and blood correlate better than hepatocyte growth factor with hepatocyte proliferation during liver regeneration. Am J Physiol 1998;153:955–61.

Webber EM, Godowski PJ, Fausto N. In vivo response of hepatocytes to growth factors requires an initial priming stimulus. Hepatology 1994;14:489–97.

Wolpert MK, Althaus JR, Johns DG. Nitroreductase activity of mammalian liver aldehyde oxidase. J Pharmacol Exp Ther 1973;185:202–13.

Zafarullah M, Li WQ, Sylvester J, et al. Molecular mechanisms of *N*-acetylcysteine actions. Cell Mol Life Sci 2003;60:6–20.

Exp Toxic Pathol 2004; **55**: 325–330
http://www.elsevier-deutschland.de/etp

Department of Veterinary Pathology, Graduate school of Agricultural and Life Science, The University of Tokyo, Japan

Rat strain differences in the early stage of porcine-serum-induced hepatic fibrosis

YASUKO BABA, KOJI UETSUKA, HIROYUKI NAKAYAMA, and KUNIO DOI

With 10 figures

Received: July 14, 2003; Revised: September 11, 2003; Accepted: October 1, 2003

Address for correspondence: YASUKO BABA, Department of Veterinary Pathology, Graduate school of Agricultural and Life Science, The University of Tokyo, 1-1-1, Yayoi, Bunkyo-ku, Tokyo 113-8657, Japan; Tel.: ++81-3-5841-5401, Fax: ++81-3-5841-8185, e-mail: aa27157@mail.ecc.u-tokyo.ac.jp

Key words: Porcine serum; Brown Norway rat; Sprague Dawley rat; Wistar rat; hepatic fibrosis.

Summary

Rat strain differences in the early development of porcine serum (PS)-induced hepatic fibrosis were histologically and immunohistochemically examined using Brown Norway (BN), Sprague Dawley (SD) and Wistar rats. They were injected i.p. with 0.5ml sterile PS twice a week for 4 and 8 weeks. In addition, rats treated with physiological saline in the same way served as controls. At 4 weeks, hepatic fibrosis accompanying fibrous septa mainly composed of type III collagens developed in BN and SD rats but not in Wistar rats. In addition, the numbers of eosinophils, CD3-positive cells and ED-1-positive cells significantly increased in BN and SD rats, that of CD45RA-positive cells in BN rats, and that of α-smooth muscle actin (SMA)-positive cells in SD rats, respectively. Such differences in the number of inflammatory cells may be related with the absence of hepatic fibrosis in Wistar rats at 4 weeks. At 8 weeks, hepatic fibrosis with formation of many small-sized pseudolobules was observed in all strains at almost similar degree, and the numbers of infiltrating cells increased in all strains of rats with some exception. In addition, the main location of inflammatory cells was different, suggesting a different role of each inflammatory cell in the process of hepatic fibrosis.

Introduction

In human hepatic fibrosis and cirrhosis, it has been reported that fat-storing cells, i.e. Ito's cells, are activated by mediators released from injured hepatocytes, resulting in hepatic fibrosis (MARTINEX and MARTINEZ 1991), but detailed fibrogenic process and mechanisms of hepatic fibrosis are still obscure. To elucidate these points, many animal models have been developed as follows: models induced by carbon tetrachloride (AKIYOSHI and TERADA 1998; ARMBRUST et al. 1997), radiation (GERACI et al. 1992; PENG et al. 1994), diethyl nitrosamine (STEINHOFF 1975; XU et al. 1994), bile duct resection (RIOUX et al. 1996; SUGIHARA et al. 1999) and porcine serum (BALLARDINI et al. 1988; BHUNCHET et al 1996; BHUNCHET and FUJIEDA 1993; BHUNCHET and WAKE 1992; KITAMURA et al. 1984; NAKANO 1986; SENOO and WAKE 1985; SHIGA et al.1997). Differing from many post-necrotic fibrosis models, porcine-serum-induced hepatic fibrosis in rats is characterized by accompanying little hepatocyte damage (BHUNCHET and FUJIEDA 1993; BHUNCHET and WAKE 1992; FUJIWARA et al. 1988; ISHIDA et al. 1991). However, there are few reports of rat strain differences in the early development of porcine-serum-induced hepatic fibrosis. The present study was carried out to clarify this point using 3 strains of rats, i.e. Brown Norway, Sprague-Dawley and Wistar rats. Brown Norway rats are well known to show high immunoreactivities (HACZKU et al. 1995; UYAMA et al. 1995), and Sprague Dawley and Wistar rats are frequently used in toxicologic studies. The protocol of this study was approved by the Animal Care and Use Committee of Graduate School of Agricultural and Life Sciences, the University of Tokyo.

Materials and methods

Animals: Twenty 5-week-old male rats each of Brown Norway (BN/Crj) (BN) (90 ± 10g), Sprague-Dawley (Crj:CD(SD)IGS) (SD) (140 ± 10g) and Wistar strains (Crj:Wistar) (140 ± 10g) were purchased from Charles River Japan Co., Kanagawa. The animals were housed

0940-2993/04/55/05-325 $ 15.00/0

2–3 per cage using an isolator caging system (Niki Shoji Co., Tokyo) in an animal room (temperature: 23 ± 2 °C, relative humidity: 55 ± 5%, and 12 hr-light and 12 hr-dark cycle) and fed commercial pellets (MF, Oriental Yeast Co., Tokyo) and water *ad libitum*. The animals were subjected to the experiment after acclimation for one week.

Treatments: The rats of each strain were divided into two groups. One group was intraperitoneally (i.p.) injected with 0.5ml/rat of sterile porcine serum (PS) (COSMO BIO Co., Ltd) twice a week, and the other group was treated with sterile physiological saline (S) in the same way and served as controls. At 4 and 8 weeks, five rats of each group were killed by blood sampling from abdominal aorta under ether anesthesia at 24 hours (hrs) after the last PS injection.

Body and organ weights: The rats were weighed every other week. At necropsy, the liver, spleen and kidneys of each rat were also weighed, and the ratio of organ weight to body weight (relative organ weight) (g%) was calculated.

Histopathology: The liver, spleen and kidneys were fixed in 10% neutral buffered formalin. Four-μm paraffin sections were stained with hematoxylin and eosin (HE), toluidine blue (TB) or Masson's trichrome (MT), and subjected to histopathological examination. The numbers of eosinophils and mast cells in randomly selected 10 fields per rat were counted on HE- or TB-stained section under light microscopy with magnification ×400, and an average number per field was calculated for each rat.

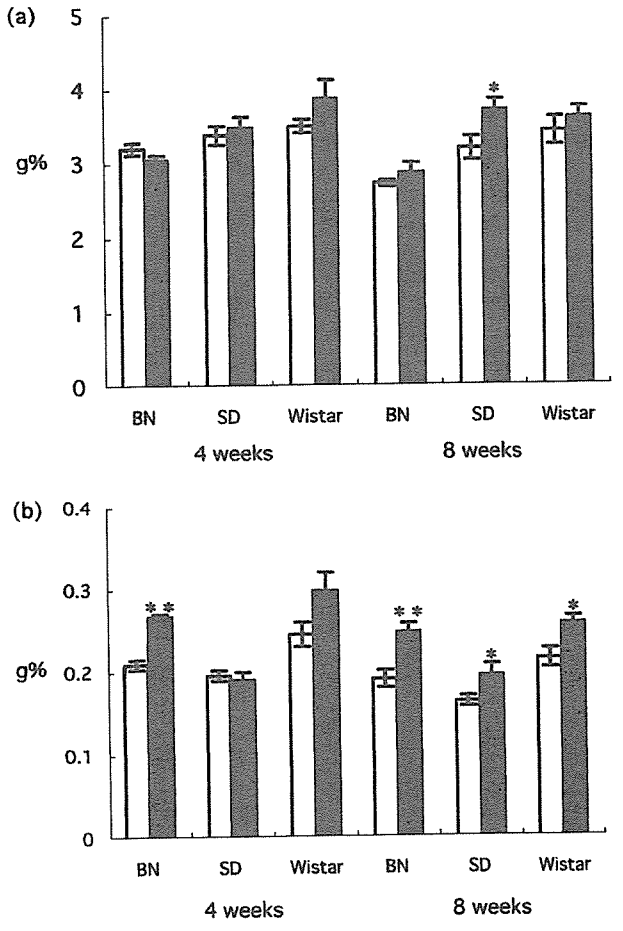

Fig. 1. Changes in the relative liver (**a**) and spleen (**b**) weights. *P < 0.05, **P < 0.01; Significantly different from Saline group.

Immunohistochemistry: For immunohistochemical examination of infiltrating cells, paraffin sections of the liver were stained by labeled streptavidin biotinylated antibody (LSAB) method. The primary antibodies used were anti-rat CD3 and CD45RA (Pharmingen, San Diego, CA, USA), anti-human alpha-smooth muscle actin (α-SMA) (DAKO, Kyoto, Japan) and anti-rat ED-1 mouse monoclonal antibodies (BMA Biochemical Ltd., Switzerland). In addition, for immunohistochemical examination of extracellular matrices, anti-rat type I collagen, anti-bovine type III collagen, anti-bovine fibronectin and anti-mouse laminin rabbit polyclonal antibodies (LSL, Tokyo, Japan) were used. Positive signals were visualized by treating with 3,3′-diaminobenzidine tetrahydrochloride and counterstain was done with hematoxylin.

The number of positive cells for each antibody was calculated as those of eosinophils and mast cells.

Statistical analysis: The body weight, relative organ weights of the liver, spleen and kidney, and the numbers of inflammatory cells were presented as mean ± standard error (SE) of 5 rats. Statistical analysis was done between PS and S groups and among 3 strains of PS group using the Student's *t*-test.

Results

Changes in body and organ weights

The change in body weight was similar between PS and S groups in all 3 strains of rats. The relative liver weight of PS group was significantly higher than that of S group at 8 weeks in SD rats (fig. 1a). The relative spleen weight of PS group was significantly higher than that of S group except for than in SD and Wistar rats at 4 weeks (fig. 1b). On the other hand, the relative kidney weight showed no significant difference between PS and S groups in all 3 strains of rats.

Histological findings

The liver of S group showed no histopathological changes. In PS group, at 4 weeks, hepatic fibrosis occurred in BN and SD rats, but not in Wistar rats. Hepatic fibrosis was somewhat severer in SD rats than in BN rats at 4 weeks (fig. 2). At 8 weeks, hepatic fibrosis with formation of many small-sized pseudolobules developed in rats of all strains at almost the similar degree (fig. 3). Positive stainabilities for type I collagen, type III collagen, fibronectin and laminin were detected in the portal tract and around the central vein, but fibrotic septa showed positive stainability only for type III collagen (fig. 4).

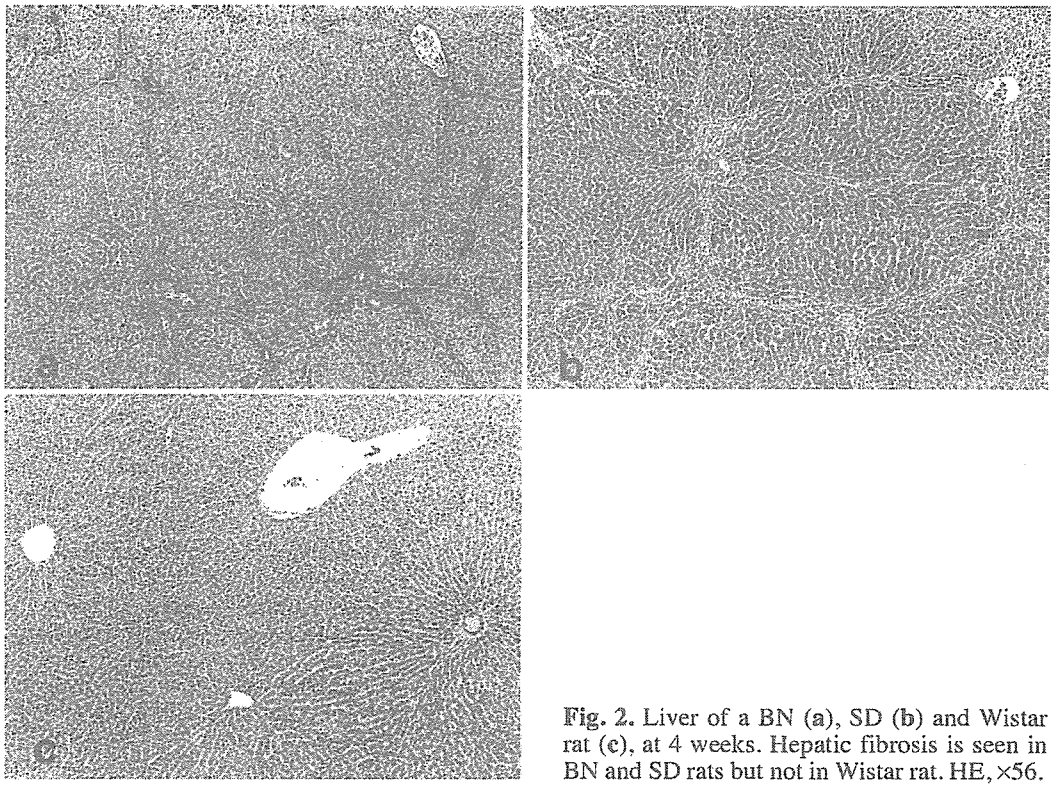

Fig. 2. Liver of a BN (a), SD (b) and Wistar rat (c), at 4 weeks. Hepatic fibrosis is seen in BN and SD rats but not in Wistar rat. HE, ×56.

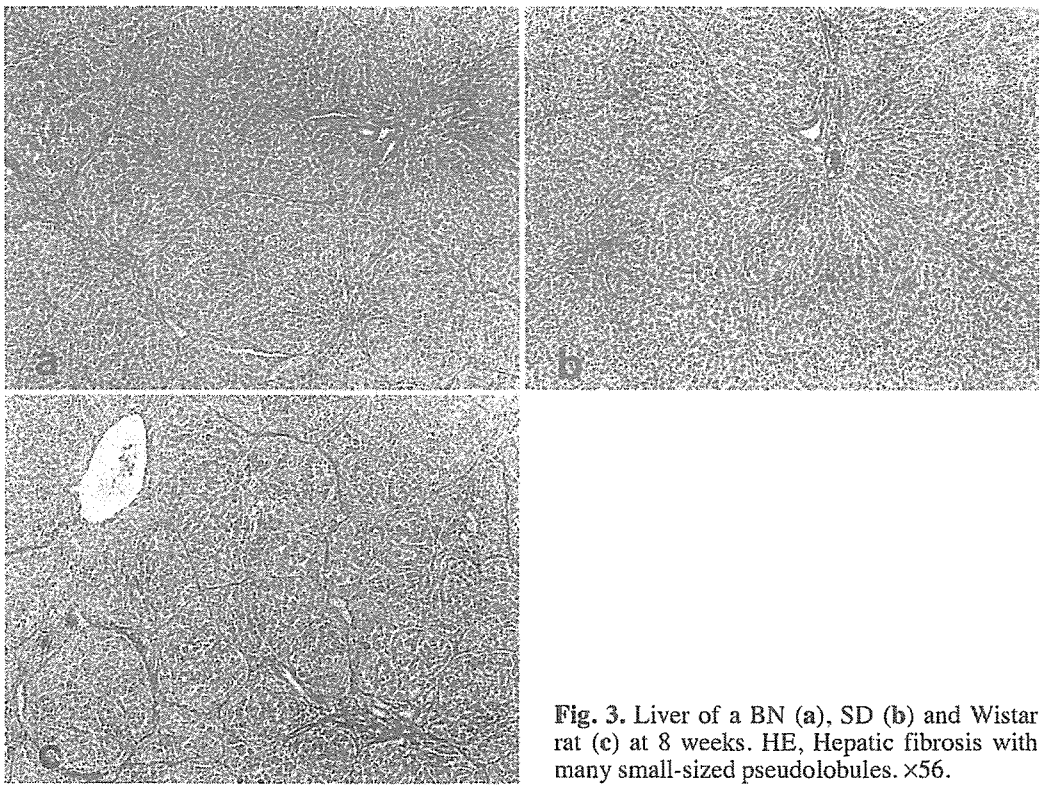

Fig. 3. Liver of a BN (a), SD (b) and Wistar rat (c) at 8 weeks. HE, Hepatic fibrosis with many small-sized pseudolobules. ×56.

In and around the portal tract, around the central vein and along the fibrous septa, infiltration of mast cells, eosinophils, and mononuclear round-shaped and spindle-shaped cells were seen in the liver of PS group except for Wistar rats at 4 weeks (fig. 5). The majority of spindle-shaped cells in the fibrous septa were positive for SMA (fig. 6), and the number of α-SMA-positive cells significantly increased only in SD rats at 4 weeks, and it significantly increased in all strains of rats at 8 weeks (fig. 7).

The number of mast cells showed a slight but significant increase in all strains at 4 weeks, and it increased prominently at 8 weeks (fig. 8a). The rate of increase in number was highest in BN rats. Except for Wistar rats at 4 weeks, the number of eosinophils significantly increased in the liver of PS group in all strains at 4 and 8 weeks (fig. 8b). Mast cells and eosinophils were mainly localized in and around the portal tract (fig. 5 Inset). The number of CD45RA-positive cells began to significantly increase at 4 weeks and it was more elevated at 8 weeks in BN rats. In Wistar rats, it increased significantly at 8 weeks (fig. 9a). Except for Wistar rats at 4 weeks, the numbers of CD3-positive cells (fig. 9b) and ED-1 positive cells (fig. 9c) significantly increased in the liver of PS group of all strains at 4 and 8 weeks. CD45RA-, CD3- and ED1-positive cells were observed in the whole area of the hepatic lobule (fig. 10).

There were few injured hepatocytes noticed throughout the experimental period.

The lymphoid follicles in the spleen of PS group showed slight hyperplasia, but the kidney showed no histological changes even in PS group of all strains throughout the experimental period.

Discussion

In the present study, rat strain differences in the early stage of PS-induced hepatic fibrosis were examined among BN, SD and Wistar rats. As a result, the progression of hepatic fibrosis was somewhat different among these strains. For example, hepatic fibrosis started at 4 weeks in BN and SD rats while it developed at 8 weeks in Wistar rats. In addition, hepatic fibrosis at 4 weeks was somewhat severer in SD rats than BN rats.

Among body and organ weights, the relative spleen weight, except for that in SD rats at 4 weeks, was significantly higher in PS group than in S group. The increased relative spleen weight seems to be related with hyperplasia of lymphoid follicles, suggesting antibody production against PS as supposed in the previous reports (IMAOKA et al. 1986). Further study on immunological responses following PS-treatments is now under progress.

Hepatic fibrosis was considered to start in and around the portal tract as well as around the central vein, and then occurred in the Disse's space, resulting in formation of fibrous septa and further establishment of pseudolobules (KITAMURA et al. 1984). Immunohistochemically, fibrous septa were mainly composed of type III collagen probably produced by α–SMA-positive cells, i.e. activated fat-storing cells.

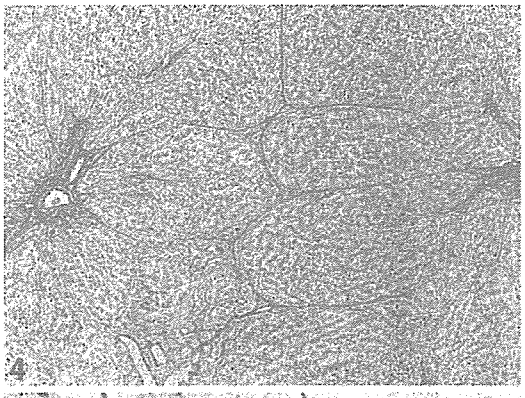

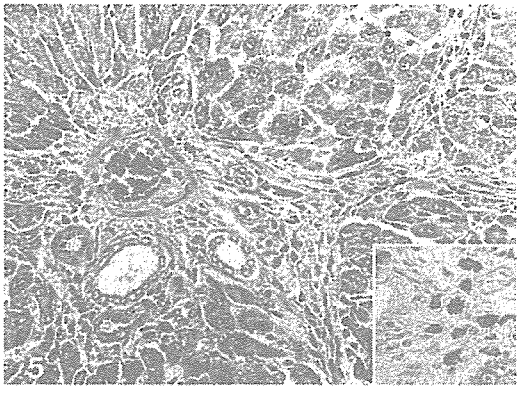

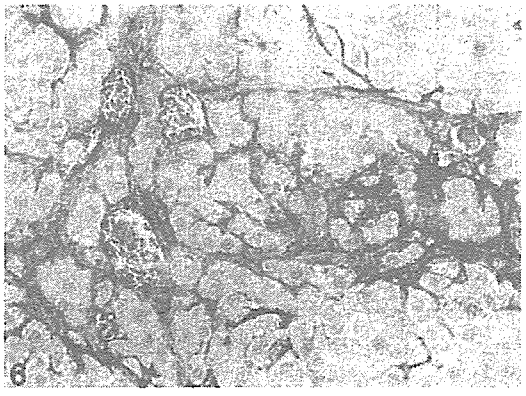

Fig. 4. Liver of a BN rat at 4 weeks. Fibrous septa are positive for type III collagen. Immunostaining, ×56.

Fig. 5. Liver of a SD rat at 4 weeks. Many inflammatory cells are seen around the portal tract and along the fibrous septa. HE, ×204. Inset: Infiltration of mast cells in the portal tract. TB, ×350.

Fig. 6. Liver of a BN rat at 8 weeks. Infiltration of α–SMA-positive cells along the fibrous septa. Immunostaining, ×231.

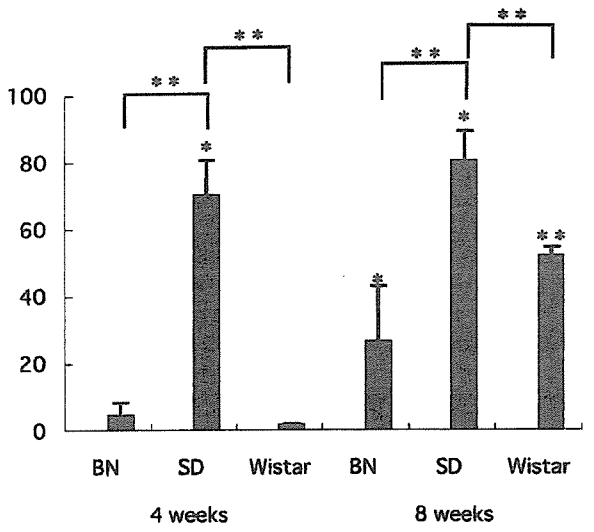

Fig. 7. Kinetics of α-SMA-positive cells in the liver of BN, SD and Wistar rats. ■: Porcine serum group. □: Saline group. *P < 0.05, **P < 0.01; Significantly different from S group or between each PS group.

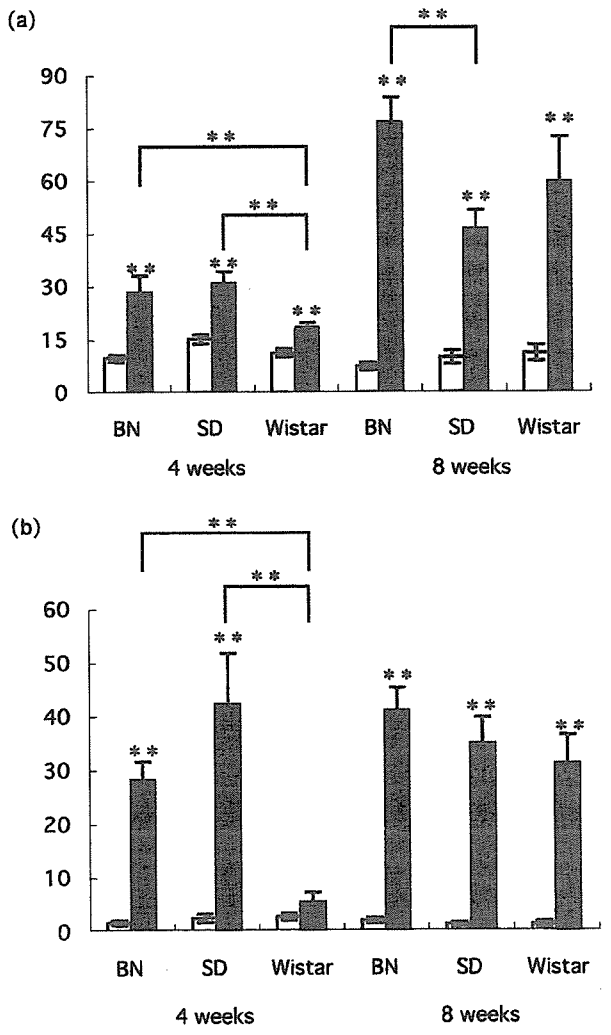

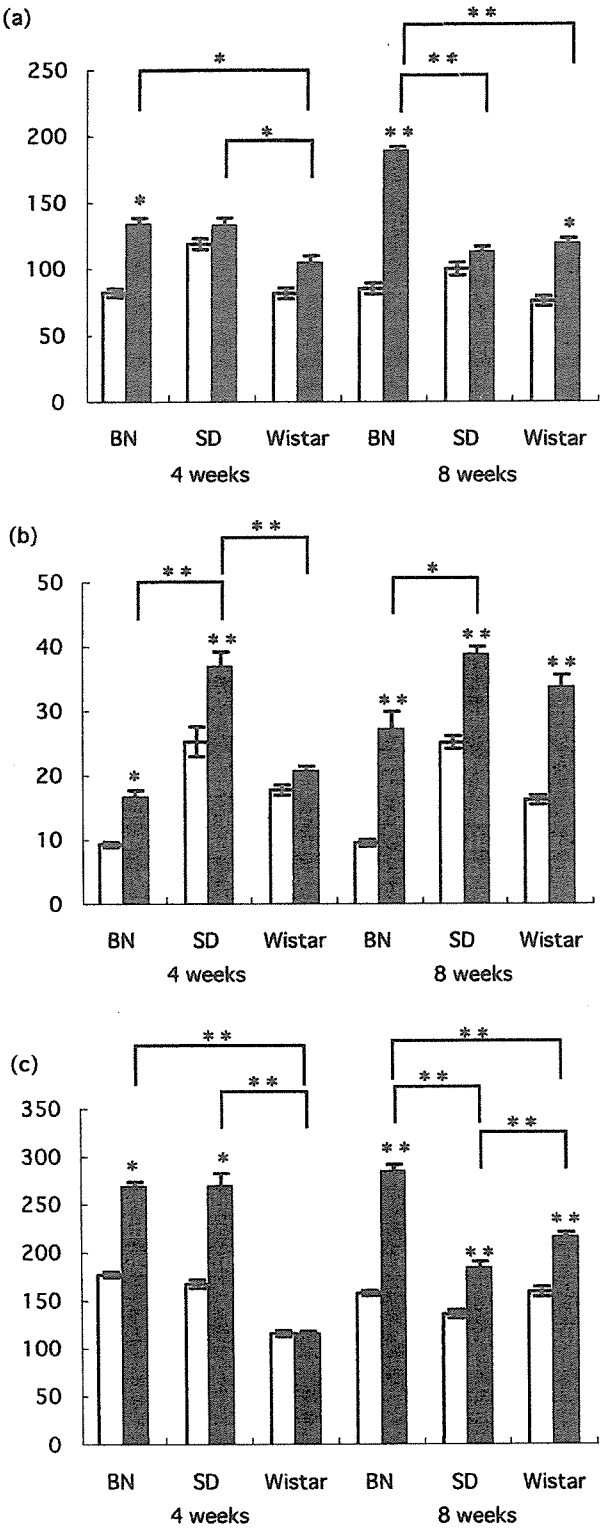

Fig. 9. Kinetics of CD45RA-positive cells (**a**), CD3-positive cells (**b**) and ED-1-positive cells (**c**) in the liver of BN, SD and Wistar rats. See the footnote of fig. 7.

◀ **Fig. 8.** Kinetics of mast cells (**a**) and eosinophils (**b**) in the liver of BN, SD and Wistar rats. See the footnote of fig. 7.

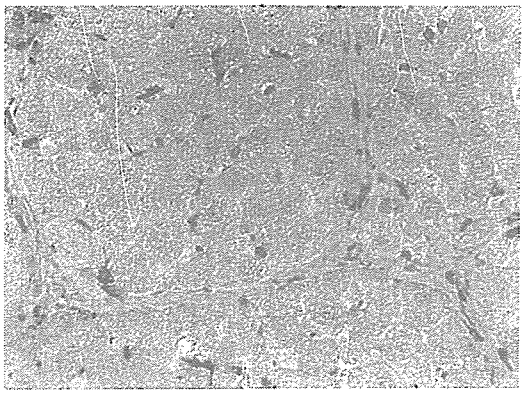

Fig. 10. Liver of a BN rat at 8weeks. ED1-positive cells are found in the whole area of hepatic lobule. Immunostaining, ×231.

The main location of each infiltrating cell in the liver differed from each other. For example, eosinophils and mast cells were localized mainly in and around the portal tract, fibroblasts in and around the portal tract as well as around the central vein, macrophages and B and T lymphocytes in the whole area of hepatic lobule, and α–SMA-positive cells in the fibrous septa, respectively. Such difference suggests that they may play a different role in the development of PS-induced hepatic fibrosis.

In contrast to those in the liver of BN and SD rats, in the liver of Wistar rats, the numbers of eosinophils, macrophages and B and T lymphocytes did not significantly increased at 4 weeks. This may be related with the absence of hepatic fibrosis in Wistar rats at 4 weeks. In addition, this also suggests that inflammatory cells may be related in the early development of PS-induced hepatic fibrosis. Further studies on immunopathological events which are supposed to be responsible for the initiation and progression of PS-induced hepatic fibrosis are now in progress.

In conclusion, there were some rat strain differences in the early stage of PS-induced hepatic fibrosis among BN, SD and Wistar rats, and such differences may be related to the severity of inflammatory cell infiltration in the liver.

References

AKIYOSHI H, TERADA T: Mast cell, myofibroblast and nerve terminal complexes in carbon tetrachloride-induced cirrhotic rat livers. J Hepatol 1998; **29**: 112–119.

ARMBRUST T, BATUSIC D, RINGE B, et al.: Mast cells distribution in human liver disease and experimental rat liver fibrosis. Indications for mast cell participation in development of liver fibrosis. J Hepatol 1997; **26**: 1042–1054.

BALLARDINI G, FALLANI M, BIAGINI G, et al.: Desmin and actin in the identification of Ito cells and in monitoring their evolution to myofibroblasts in experimental liver fibrosis. Virchows. Arch B Cell Pathol Include Mol Pathol 1988; **56** : 45–49.

BHUNCHET E, EISHI Y, WAKE K: Contribution of immune response to the hepatic fibrosis induced by porcine serum. Hepatology 1996; **23**: 811–817.

BHUNCHET E, FUJIEDA K: Capillarization and venularization of hepatic sinusoids in porcine serum-induced rat liver fibrosis: a mechanism to maintain liver blood flow. Hepatology 1993; **18**: 1450–1458.

BHUNCHET E, WAKE K: Role of mesenchymal cell population in porcine serum-induced rat liver fibrosis. Hepatology 1992; **16**: 1452–1473.

FUJIWARA K, OGATA I, OHTA Y, et al. Decreased collagen accumulation by a prolylhydroxylase inhibitor in pig serum-induced fibrotic rat liver. Hepatology 1988; **8**: 804–807.

GERACI JP, MARIANO MS, JACKSON KL: Radiation hepatology of the rat: microvascular fibrosis and enhancement of liver dysfunction by diet and drugs. Radiat Res 1992; **129**: 322–332.

HACZKU A, CHUNG KF, SUN J, et al.: Airway hyperresponsiveness, elevation of serum-specific IgE and activation of T cells following allergen exposure in sensitized Brown-Norway rats. Immunology 1995; 85: 598–603.

IMAOKA K, DOI K, DOI C, et al.: Mouse strain difference in bile duct lesions induced by swine serum injections. Lab Anim 1986; **20**: 321–324.

ISHIDA N, NAKATA K, TAKASE K, et al.: The protective effects of SA3443, a novel cyclic disulfide, on chronic liver injuries in rats. J Hepatol 1991; **13**: 200–207.

KITAMURA K, YASOSHIMA A, IWASAKI OH, et al.: Hepatic fibrosis produced in rats by repeated intraperitoneal injections of swine serum. Jpn J Vet Sci 1984; **46**: 265–271.

MARTINEX HA, MARTINEZ J: The role of capillarization in hepatic failure: studies in carbon tetrachloride–induced cirrhosis. Hepatology 1991; **14**: 864–874.

NAKANO M: Early morphological changes of porcine serum-induced hepatic fibrosis. Acta Pathol Jpn 1986; **36**: 415–422.

PENG RY, WANG DY, XU ZH, et al.: The changes and significance of mast cells in irradiated rat liver. J Environ Pathol Toxicol Oncol 1994; 44: 655–661.

RAPPAPORT AM: The structural and functional unit in the human liver (liver acinus). Anat Rec 1958; **130**: 637–686.

RIOUX KP, SHARKEY KA, WALLACE JL, et al.: Hepatic mucosal mast cell hyperplasia in rats with secondary biliary cirrhosis. Hepatology 1996; **23**: 888–895.

SENOO H, WAKE K: Suppression of experimental hepatic fibrosis by administration of vitamin A. Lab Invest 1985; **52**: 182–194.

SHIGA A, SHIROTA K, IKEDA T, et al.: Morphological and immunohistochemical studies on porcine serum-induced rat liver fibrosis. J Vet Med Sci 1997; **59**: 159–167.

STEINHOFF D: Effect of diethylnitrosamine on the livers of rats after high oral doses administered at intervals varying between three and twenty-four days. Acta Hepatogastroenterol (Stuttg) 1975; **22**: 72–77.

SUGIHARA A, TUJIMURA T, FUJITA Y, et al.: Evaluation of role of mast cells in the development of liver fibrosis using mast cell-deficient rats and mice. J Hepatol 1999; **30**: 859–867.

UYAMA O, IHAKU D, KITADA O, et al.: Role of eosinophils and cell adhesion molecules in the allergen-induced asthmatic response of rats. Res Commun Mol Pathol Pharmacol 1995; **90**: 3–15

XU X, RUAN YB, WU ZB: Study on the role of mast cells in the development of liver fibrosis during diethylnitrosamine (DEN)-induced hepatocarcinogenesis in rats. J Tongji Medical University 1994; **14**: 193–199.

Available online at www.sciencedirect.com
SCIENCE DIRECT®
ELSEVIER
Experimental and Toxicologic Pathology 56 (2005) 235–244
EXPERIMENTAL AND TOXICOLOGIC PATHOLOGY
www.elsevier.de.etp

Gene expression profiling in streptozotocin treated mouse liver using DNA microarray

Eisuke Kume[a,*], Chinami Aruga[a], Yukito Ishizuka[a], Kaori Takahashi[a], Satoko Miwa[a], Masahito Itoh[a], Hisako Fujimura[a], Wataru Toriumi[a], Kazuyuki Kitamura[b], Kunio Doi[c]

[a]*Exploratory Toxicology and DMPK Research Laboratory, Tanabe Seiyaku Co. Ltd., 2-2-50, Kawagishi, Toda, Saitama 335, Japan*
[b]*Safety Research Laboratory, Tanabe Seiyaku Co. Ltd., Osaka, Japan*
[c]*Department of Veterinary Pathology, Graduate School of Agricultural and Life Sciences, The University of Tokyo, Tokyo, Japan*

Received 9 August 2004; received in revised form 9 September 2004; accepted 22 September 2004

Abstract

Streptozotocin (SZ) is known to exert toxic effects not only on pancreatic islet beta cells but also on other organs including liver. For analyzing changes in genes expression associated with SZ toxicity, we performed DNA microarray analyses on the liver obtained from SZ-treated mice. Eight-week-old male ICR mice were treated i.p. with 200 mg/kg of SZ, and the blood and liver were taken at 6, 24 and 48 h after the treatment. Labeled cRNA prepared from total RNA of the liver was hybridized to the GeneChip Murine Genome U74A V.2 (Affymetrix). The number of the probe sets, which were clearly up-regulated or down-regulated, were over 100 at 6 and 24 h after the SZ-treatment, and it decreased at 48 h after the treatment. Many of the up-regulated genes were categorized into cell cycle/apoptosis related genes, immune/allergy related genes and stress response/xenobiotic metabolism related genes. On the other hand, genes related to glucose, lipid and protein metabolisms were down-regulated. These changes started prior to the elevation of the serum glucose levels, indicating the direct action of SZ on the liver rather than the secondary effect of diabetes. This may be related with the previously reported hepatic changes such as lipid peroxidation, mitochondrial swelling and inhibition of hepatocyte proliferation observed before the development of hyperglycemia (Exp. Toxic Pathol. 55 (2004) 467)

Keywords: Streptozotocin; Diabetes; Hepatic alteration; Gene expression; DNA microarray; Mouse

Introduction

Although streptozotocin (SZ), an extract from *Streptomyces achromogenes*, was originally developed as an antibiotic and/or antitumor agent (Vavra et al., 1960; White, 1963), it has been attracting a great attention as a useful tool for the induction of diabetes mellitus and its complications in laboratory rodents (Sibay et al., 1971; Steffes and Mauer, 1984; Kume et al., 1992) because of its toxic action on islet ß cells. We have previously reported the details of SZ-induced hepatic lesions in the acute (6–48 h after the treatment) and the subacute (4–12 weeks after the treatment) phase (Kume et al., 1994a,b; Doi et al., 1997, Kume et al., 2004). Those studies characterized the pathological changes such as the appearance of oncocytic hepatocytes, cytomegalic

*Corresponding author. Tel.: +81 48 433 8122; fax: +81 48 433 8171.
E-mail address: e-kume@tanabe.co.jp (E. Kume).

0940-2993/$ - see front matter © 2004 Elsevier GmbH. All rights reserved.
doi:10.1016/j.etp.2004.09.002

hepatocytes and bile duct hyperplasia in the subacute phase. In addition, it was also clarified that several hepatic changes including lipid peroxidation, mitochondrial swelling, peroxisome proliferation and inhibition of hepatocyte proliferation occurred before the elevation of the serum glucose levels, which indicated that those changes were attributable to the direct effects of SZ on hepatocytes rather than the secondary effects of diabetes or hyperglycemia (Kume et al., 2004).

Several reports have focused on the molecular genetic effects associated with SZ-induced diabetes (Wada et al., 2001; Dhahbi et al., 2003; Susztak et al., 2004); however, no researchers reported the changes in genes expression in SZ-treated animals before they showed hyperglycemia. This study, using the Affymetrix GeneChip, revealed molecular genetic changes in the liver before (6 and 24 h after the treatment) and after (48 h after the treatment) the induction of hyperglycemia.

Materials and methods

The study was approved by the Ethical Committee at Tanabe Seiyaku Co., Ltd. and all efforts were made to minimize animal suffering.

Animals and treatments

Eighteen 8-week-old male Crj:CD-1(ICR) mice (Charles River Japan Inc., Kanagawa, Japan) were used. The animals were housed in polycarbonate cages in a barrier system animal room under controlled conditions (temperature: 23 ± 2 °C, humidity: 55 ± 5%, 12 h light/dark cycle) and fed CRF-1 pellets (Oriental Yeast Co. Ltd. Tokyo, Japan) and tap water ad libitum throughout the experimental period. Half of the animals (three groups of three mice) were injected intraperitoneally with 200 mg/kg b.w. of SZ (Sigma, St. Louis, MO, USA) at around 9:00 a.m. SZ was dissolved in 0.05 M citrate buffer solution (pH 4.5) just before used. At 6, 24 and 48 h after SZ-injections, whole blood was taken from the *aorta abdominalis* of the three mice in each group under ether anesthesia. After that, the livers were removed and the small pieces of the left lateral lobe of the liver were quickly frozen. The other nine mice, which were given vehicle alone and killed in the same way, served as vehicle controls.

RNA extraction

Total liver RNA was isolated from the frozen tissue fragments using ISOGEN reagent (Nippon Gene, Tokyo, Japan). The RNA fractions from the three mice in each group were pooled for GeneChip analysis.

Affymetrix GeneChip analysis

Pooled total RNA from each group was labeled as described in the GeneChip Expression Analysis Technical Manual (Affymetrix, Santa Clara, CA). mRNA was reverse-transcribed into cDNA using SuperScript Choice system (Invitrogen Life Technologies) and T7-(dT) 24 primer (Amersham Biosciences, Piscataway, NJ). The cDNA was converted to labeled cRNA using Bioarray HighYield RNA Transcript Labeling Kit (Affymetrix), which was purified using RNeasy Mini Kit (QIAGEN, Valencia, CA). The labeled cRNA was hydrolyzed in fragmentation buffer (40 mM Tris-acetate pH8.1, 100 mM KOAc, 30 mM MgOAc) to a size of approximately 35-200 nucleotides.

Ten microgram of the fragmented cRNA was hybridized with the Murine Genome U74AV2 array (Affymetrix) in hybridization cocktail (0.05 ug/uL cRNA, 50 pM control oligonucleotide B2, 1.5 pM bioB, 5 pM bioC, 25 pM bioD, 100 pM cre, 0.1 mg/mL herring sperm DNA, 0.5 mg/mL acetylated BSA, 100 mM MES, 1 M Na+, 20 mM EDTA, 0.01% Tween20). Hybridization was carried out overnight (16 h) at 45 °C, followed by washing, and staining with streptavidin-phycoerythrin (SAPE, Molecular Proves, Eugene, OR). Hybridization assay procedures including preparation of solutions were carried out as described in the Affymetrix GeneChip Expression Analysis Technical Manual. The distribution of fluorescent material on the array was determined using a confocal laser scanner (GeneArray Scanner, Affymetrix).

Array data processing

Signal quantification, background adjustment, judgment of detection call and other analysis were performed using the Microarray Suite (MAS) ver. 5.0 (Affymetrix). All arrays were globally scaled to a target value of 200. Genes were only considered for further analysis, if their corresponding probe sets had a signal intensity over 300 and their detection call was P (present). Pair-wise comparison analysis was performed between SZ-treated mice and control mice. The signal log ratio (SLR) was calculated for each probe set using the following formula: $\log_2$ (signal intensity in SZ-treated mice/that in control mice). Probe sets with SLR greater or equal to 1.0 was judged as 'up-regulated'. On the other hand, probe sets with SLR less or equal to -1.0 was judged as 'down-regulated'.

Annotation information on the probe sets on the U74A V.2 array was downloaded from the NetAffyx provided by Affymetrix. The probe sets judged as 'up-regulated' or 'down-regulated' were categorized according to the annotation information and protein information from Protein Knowledgebase provided by Swiss Institute of Bioinformatics (Swiss-Prot).

Signal transduction relationship between the up- or down-regulated genes was looked over and graphically displayed, using a database TransPath (BioBase, Wolfenbüttel Germany) accessorily. That analysis was performed exploratory without regard for the SLR.

Reverse transcription-polymerase chain reaction (RT-PCR)

The expressions of 10 genes were examined by RT-PCR to confirm the results of the GeneChip analysis. For GADD 45, Mdm2, Bcl2l, Wig1, Bax, Cdkn1a, Ppara, Srebf1, Hmgcs2 and Trp53, samples from 6 h after the treatment were used, and samples from 24 h after the treatment was used for Scd1, according to the results of the GeneChip analysis.

Frozen livers were thawed on ice, and total RNA was isolated using ISOGEN reagent. The quality of the isolated RNA was assessed by electrophoresis on RNA 6000 Nano kit (Agilent Tech.) based on the integrity of 28S and 18S bands.

The forward and reverse primers were designed using Primer Express software version 1.5 (Applied Biosystems) from the mouse mRNA sequence. The mRNA sequences were obtained from nr (All GenBank + RefSeq Nucleotides + EMBL + DDBJ + PDB sequences (but no EST, STS, GSS, or phase 0, 1 or 2 HTGS sequences). No longer "non-redundant"). Each primer was homology searched by NCBI BLAST search to ensure that it was specific for the target mRNA transcript. The primers were synthesized by QIAGEN K.K. (Tokyo, Japan).

RT-PCR were conducted in one step using the SYBR® Green RT-PCR Kit in a ABI PRISM 7700 Sequence Detector system (Applied Biosystems) according to the manufacturer's protocol.

Samples were deemed positive at any given cycle when the value of the emitted fluorescence was greater than the threshold value calculated by the instrument's software (Sequence Detector Ver.1.6.3). The threshold cycle, which is defined as the cycle at which PCR amplification reaches a significant value (i.e., usually 15 times the standard deviation of the baseline), is given as a mean value.

The data are expressed as the ratio of target mRNA to GAPDH mRNA, and the data are then shown as a fold change relative to control at each time point.

Results

Comparison analysis of the expression profiles was performed between SZ-treated mice and control mice from the GeneChip data. Fig. 1 shows the number of the up-regulated (SLR $\geq$ 1.0) or the down-regulated (SLR $\leq$ −1.0) probe sets in the liver of SZ-treated mice. The number of probe sets, which were clearly up-regulated or down-regulated, was over 100 at 6 and 24 h after the SZ-treatment, and it decreased at 48 h after the treatment. There were only a small number of genes which showed similar changes among the time points examined.

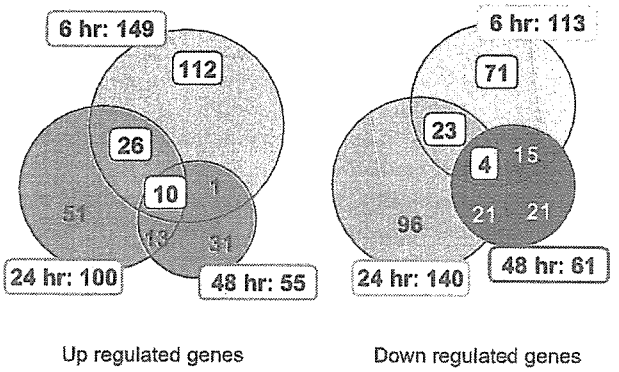

Fig. 1. Up- or down-regulated probe sets in the liver of the SZ-treated mice. Condition: Up regulation: signal $\log_2$ ratio to control group $\geq$ 1, signal intensity > 300. Down regulation: signal $\log_2$ ratio to control group $\leq$ −1, signal intensity of control group > 300.

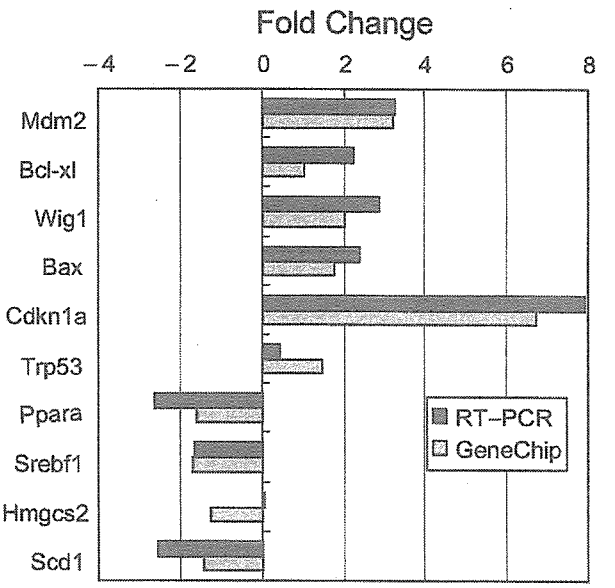

Fig. 2. Validation of the GeneChip data with RT-PCR. The expression of 11 genes was analyzed using GeneChip and RT-PCR. The changes in the expression of these genes were similar in the direction and the magnitude between the two techniques.

Probe sets, of which SLR was over 1.5 or was under −1.5, were picked up and tabulated in Table 1. Genes corresponding to those probe sets were categorized according to the information mainly from the

Table 1. Hepatic gene expression in the streptozotocin treated mice

Title	GeneName	6hr	24hr	48hr	Affy ID
Carbohydrate and lipid metabolism					
amylase 2, pancreatic	Amy2		0.5		97524_f_at
amylase 2, pancreatic	Amy2		-0.5		97523_i_at
apolipoprotein A-IV	Apoa4	0.5	0.7		100078_at
carboxyl ester lipase	Cel		-0.1		99939_at
carboxylesterase 1	Ces1		1.2	0.1	103519_at
colipase, pancreatic	Clps	-1.1			160132_at
cytosolic acyl-CoA thioesterase 1	Cte1			0.8	103581_at
cytochrome P450, family 7, subfamily a, polypeptide 1	Cyp7a1	-0.7	-0.9		99404_at
cytochrome P450, family 8, subfamily b, polypeptide 1	Cyp8b1	-1.4		-0.6	103284_at
fatty acid synthase	Fasn	0.9		-0.2	98575_at
farnesyl diphosphate synthetase	Fdps	0.4		0.3	160424_f_at
farnesyl diphosphate synthetase	Fdps	0.4		-0.2	98098_at
glucokinase	Gck	-0.6			102651_at
3-hydroxy-3-methylglutaryl-Coenzyme A synthase 1	Hmgcs1	-0.9		0	94325_at
3-hydroxy-3-methylglutaryl-Coenzyme A synthase 2	Hmgcs2	-0.9		-1.2	92590_at
isopentenyl-diphosphate delta isomerase	Idi1	-0.3		-0.1	96269_at
lipase, hepatic	Lipc	-0.6		-1.2	98962_at
low density lipoprotein receptor-related protein 1	Lrp1		-0.4	-0.1	101073_at
nuclear receptor subfamily 0, group B, member 2	Nr0b2		-0.8	-0.5	97123_at
NAD(P) dependent steroid dehydrogenase-like	Nsdhl	-0.1		0	98631_g_at
phosphatidylinositol 3-kinase, regulatory subunit, polypeptide 1 (p85 alpha)	Pik3r1		0.2	0.2	96592_at
phospholipid scramblase 1	Plscr1		0.1	0	102839_at
pancreatic lipase related protein 1	Pnliprp1		1.4		92601_at
peroxisome proliferator activated receptor alpha	Ppara		-0.2	0.3	102668_at
sterol-C4-methyl oxidase-like	Sc4mol	-0.9		0.2	160386_at
stearoyl-Coenzyme A desaturase 1	Scd1	-0.4	-1.4		94056_at
stearoyl-Coenzyme A desaturase 1	Scd1	-0.4			94057_g_at
sterol regulatory element binding factor 1	Srebf1		-1.1	-0.6	93264_at
thyroid hormone responsive SPOT14 homolog (Rattus)	Thrsp	-0.2		0.7	160306_at
Protein/amino acid metabolism					
betaine-homocysteine methyltransferase	Bhmt	0.1		-0.3	94049_at
carboxylesterase 3	Ces3		-1.2	-1.3	101539_f_at
carnitine palmitoyltransferase 1, liver	Cpt1a		0.1	1.2	93320_at
cysteine sulfinic acid decarboxylase	Csad	-1		-1.3	99184_at
elastase 1, pancreatic	Ela1	-0.6			93783_at
elastase 2	Ela2	-1.2	0.1		94037_at
F-box only protein 21	Fbxo21			0.5	104109_at
guanidinoacetate methyltransferase	Gamt	-0.5		-0.6	101408_at
histidine ammonia lyase	Hal		-1.1	-0.5	92833_at
homocysteine-inducible, endoplasmic reticulum stress-inducible, ubiquitin-like domain member 1	Herpud1		-0.7	-0.8	95057_at
murinoglobulin 1	Mug1	-0.9		-0.7	92837_f_at
protein tyrosine phosphatase, receptor type, D	Ptprd		-1	0.2	93485_at
tyrosine aminotransferase	Tat	-0.1		-0.7	96326_at
trypsin 2	Try2		0.8		92873_f_at
trypsin 4	Try4				101043_f_at
Cell cycle/apoptosis					
B-cell translocation gene 2, anti-proliferative	Btg2			0.8	101583_at
cyclin D1	Ccnd1	-0.3	1.2	0.5	94232_at
cyclin G1	Ccng1				160127_at
cyclin-dependent kinase inhibitor 1A (P21)	Cdkn1a				94881_at
cyclin-dependent kinase inhibitor 1A (P21)	Cdkn1a				98067_at
dual specificity phosphatase 6 (MKP3)	Dusp6			1.4	93285_at
early growth response 1	Egr1		0		98579_at
etoposide induced 2.4 mRNA	Ei24	0.8		0.8	99629_at
G0/G1 switch gene 2	G0s2	-1.2		-0.1	97531_at
Jun-B oncogene	Junb		1.3	0.9	102362_i_at
transformed mouse 3T3 cell double minute 2	Mdm2				98110_at
nucleolar protein 1	Nol1		0	-0.1	96804_at
p53 apoptosis effector related to Pmp22	Perp-pending	0.1		0.5	97825_at
serum-inducible kinase	Snk			1.4	92310_at
transducer of ErbB-2.1	Tob1	0.8			99532_at
Bcl2-associated X protein	Bax			1.1	93536_at
Tnf receptor associated factor 4	Traf4		0.1	0.1	162462_at
wild-type p53-induced gene 1	Wig1				92262_at
Immune and inflammation					
ras homolog gene family, member AB	Arhb			0.8	101030_at
chemokine (C-X-C motif) ligand 1	Cxcl1			-0.1	95349_g_at
chemokine (C-X-C motif) ligand 1	Cxcl1			-0.1	95348_at
chemokine (C-X-C motif) ligand 12	Cxcl12			-0.7	100112_at
intercellular adhesion molecule	Icam1			0.9	96752_at
interferon-stimulated protein	Isg15	0.5	1.1		98822_at
lymphocyte antigen 6 complex, locus D	Ly6d	0.9		0.8	160553_at

Continued

Table. 1 *(continued)*

Title		GeneName	6hr	24hr	48hr	Affy ID
	mannose binding lectin, serum (C)	Mbl2	1.1	2.1	1.7	97427_at
	nuclear, factor, erythroid derived 2, like 2	Nfe2l2	1.9	1.9	1.7	92562_at
	nuclear factor I/B	Nfib	2	-0.7	0	99440_at
	orosomucoid 2	Orm2	0.3	1.2	1.6	94734_at
	polymeric immunoglobulin receptor	Pigr	-0.8	2.1	-1.2	99926_at
	S100 calcium binding protein A11 (calizzarin)	S100a11	1.1	2.3	1.1	98600_at
	serine (or cysteine) proteinase inhibitor, clade A, member 6	Serpina6	-0.7	2.4	-1.1	96227_at
	serine (or cysteine) proteinase inhibitor, clade F), member 1	Serpinf1	-0.2	-0.8	2.3	93574_at
	transporter 1, ATP-binding cassette, sub-family B (MDR/TAP)	Tap1	2	1.1	0.9	103035_at
Stress response and xenobiotic metabolism						
	cytochrome P450, family 1, subfamily a, polypeptide 2	Cyp1a2	-0.1	-0.8	2.2	102998_at
	cytochrome P450, family 2, subfamily b, polypeptide 10	Cyp2b10	1.6	-0.7	-0.6	102701_at
	cytochrome P450, family 2, subfamily b, polypeptide 9	Cyp2b9	0.3	0.3	2.3	101862_at
	flavin containing monooxygenase 3	Fmo3	1.1	2.1	2.4	104421_at
	heat shock protein 1B	Hspa1b	-1.1	1.5	0.3	100946_at
	nicotinamide N-methyltransferase	Nnmt	2.3	1.2	0.4	101473_at
	serum amyloid A 2	Saa2	1.4	-0.4	2.3	103465_f_at
	serum amyloid A 3	Saa3	1.5	2	0.8	102712_at
	thioether S-methyltransferase	Temt	-1.3	3.3	2.3	97402_at
	thioredoxin-like 2	Txnl2	0.4	1.6	1	95696_at
Cytoskelton etc.						
	actin, gamma, cytoplasmic	Actg	1.5	0.5	0.4	96573_at
	cadherin 2	Cdh2	2.1	-0.2	0.3	102852_at
	gephyrin	Gphn	1	-0.6	0.1	99441_at
	p300/CBP-associated factor	Pcaf	1.6	-0.4	-0.2	104070_at
	tubulin, beta 2	Tubb2	1.5	0.2	-0.6	94835_f_at
	tubulin, beta 3	Tubb3	2	1.4	0.1	160462_f_at
Miscellaneous						
	S-adenosylhomocysteine hydrolase	Ahcy	-0.1	1.3	-0.2	96024_at
	aminolevulinic acid synthase 2, erythroid	Alas2	2.4	-0.2	-0.6	92768_s_at
	angiogenin	Ang	0.6	1.6	1	94392_f_at
	aquaporin 8	Aqp8	0	-1.2	1.6	102200_at
	ATPase, H+ transporting, V1 subunit D	Atp6v1d	0.5	2.5	1.7	96951_at
	bystin-like	Bysl	1.6	-0.1	0.1	160227_s_at
	carbonic anhydrase 14	Car14	-0.1	1.6	-0.7	98079_at
	carbonic anhydrase 3	Car3	-0.6	2.3	-0.8	160375_at
	carbonic anhydrase 5a, mitochondrial	Car5a	-0.8	2.2	-0.4	98137_at
	CCR4 carbon catabolite repression 4-like (S. cerevisiae)	Ccrn4l	0	1.3	1	99535_at
	calcitonin gene-related peptide-receptor component protein	Crcp	1.3	0.3	0.6	103334_at
	D site albumin promoter binding protein	Dbp	2.1	2.3	2.3	160841_at
	deiodinase, iodothyronine, type I	Dio1	2.5	1.9	2.1	95552_at
	Down syndrome critical region homolog 1 (human)	Dscr1	2.3	0.8	0.7	100555_at
	ectonucleotide pyrophosphatase/phosphodiesterase 2	Enpp2	1.6	-0.8	-0.3	97317_at
	UDP-N-acetyl-alpha-D-galactosamine:(N-acetylneuraminyl)-galactosylglucosylceramide-beta-1, 4-N-acetylgalactosaminyltransferase	Galgt1	1.6	-0.4	-0.2	103367_at
	glial cell line derived neurotrophic factor family receptor alpha 1	Gfra1	1.5	-0.5	0.1	93872_at
	growth hormone receptor	Ghr	1.7	-1	-0.5	99107_at
	hemoglobin alpha, adult chain 1	Hba-a1	0.9	-0.6	2.2	94781_at
	hemoglobin, beta adult major chain	Hbb-b1	1	-0.6	2.3	103534_at
	hemoglobin, beta adult major chain	Hbb-b1	0.8	-0.4	2	101869_s_at
	insulin-like growth factor binding protein 2	Igfbp2	-0.5	2.7	0	98627_at
	inositol 1,4,5-triphosphate receptor 5	Itpr5	2.5	-0.3	-0.2	101441_i_at
	kallikrein 6	Klk6	2.1	1.5	2.5	100061_f_at
	lipin 1	Lpin1	-0.1	1.4	1.6	98892_at
	nucleolar protein 5A	Nol5a	2.5	0.3	0.4	95109_at
	nuclear receptor subfamily 1, group D, member 2	Nr1d2	-0.4	1.2	2.5	99076_at
	regenerating islet-derived 1	Reg1	2.1	0.4	2.5	160213_at
	v-rel reticuloendotheliosis viral oncogene homolog A (avian)	Rela	1.5	0.2	-0.5	97813_at
	renin 1 structural	Ren1	3.5	1.2	2.6	98480_s_at
	sodium channel, voltage-gated, type I, beta polypeptide	Scn1b	0.6	2.5	1.9	102808_at
	syncollin	Sycn	-1.1	-0.1	2.5	95509_at
	thyrotroph embryonic factor	Tef	-0.1	1.3	2	160117_at

Data is shown as signal $\log_2$ ratio to each control group.

Swiss-Prot, although the genes, of which annotation was unclear (EST etc.), were excluded from the table.

The regulated genes showed a broad range, but many of the up-regulated genes were categorized into cell cycle/apoptosis related genes, immune/allergy related genes and stress response/xenobiotic metabolism related genes. On the other hand, many of the down-regulated genes belonged to glucose, lipid and protein metabolism related genes.

Ten genes were picked up among the up- or the down-regulated genes judged from GeneChip data, and were also analyzed by RT-PCR. Fig. 2 shows the fold changes

of each gene expression in SZ-treated mice from that in control mice analyzed by the GeneChip and the RT-PCR. The changes in these genes expression were similar in the direction and the magnitude between the two techniques. Only the expression changes of Hmgcs2 were different by using the RT-PCR and by using the GeneChip.

Discussion

Gene expression analysis was performed on the SZ-treated mouse liver in the acute phase of the treatment.

Affymetrix oligonucleotide microarrays generally yield data with a high degree of reliability as judged by Northern blot or quantitative PCR (Cao et al., 2001; Dhahbi et al., 2003). The changes in the expression of the 9 of 10 genes were similar in direction and magnitude between the two techniques as shown in Fig 2. Thus, we judged the GeneChip data were enough reliable, and we will discuss the expression profiles using the GeneChip data hereinafter. However, even only one gene (Hmgcs2) showed different results between the two techniques, when we pick up particular gene, quantitative PCR or other techniques should be used.

The number of up-regulated or down-regulated genes was over 100 at 6 and 24 h after the treatment. However, unexpectedly, there were only a small number of genes which showed similar changes among the time points examined. Judging from the clinicopathological examinations reported before, the 6 h after the administration was the stage when the temporal hypoglycemia was induced by an abrupt and transient insulin release from the injured pancreatic islets (Kume et al., 2004). In histopathological analysis, hepatocytes showed degenerative changes at 6 h, and they became almost normal at 24 or 48 h after the administration (Kume et al., 2004). Thus, the pathological condition seemed to be dynamically changing from 6 to 48 h after the administration, and this may explain why there were only a few genes showing similar changes among the time points examined.

Many of the up-regulated genes were categorized into cell cycle/apoptosis related genes, immune/allergy related genes and stress response/xenobiotic metabolism related genes. On the other hand, many of the down-regulated genes belonged to glucose, lipid and protein metabolism related genes. From the data, we found out the relation and the transduction pathway using a signal transduction pathway analyzing software TransPath, and the hypothetical transduction pathways were figured.

Fig. 3 indicates the relationship between the changes in apoptosis related genes expression. Numeral represents the SLR (the signal of the probe sets of the SZ treated mice/the control mice) at the corresponding time. Bcl2-associated X protein (bax), BCL2-like 11 (Bcl2l11) and other related genes were up-regulated from 6 to 48 h after the administration. Those genes belonged to Bcl2 family and were known to work on apoptosis acceleration (LeBlanc et al., 2002, O'Connor et al., 1998). Apoptotic protease activating factor 1 (Apaf1), which is known to mutually act with those genes (Robles et al., 2001), was also activated. Apaf1 interacts with caspase-9 and induces apoptosis (Cecconi et al., 1998). Moreover, p53, one of the main transcriptional factors of apoptosis (Kaelin, 1999), was up-regulated about two times at 6 h after the administration, and some of the up-regulators of p53 including 'p53 apoptosis effector related to Pmp22' (perp), wild-type p53-induced gene 1 (wig1) (Hellborg et al., 2001), and transformed mouse 3T3 cell double minute 2 (mdm2) (Gottlieb et al., 2002) were also up-regulated. Thus, the activation of apoptosis is expected. On the other hand, the up-regulation of bcl-xl and bag3, which were known to act as an inhibitor of apoptosis (Schott et al., 1995; Lee et al., 1999), was also observed. This may be related with the pathological findings of no increase in apoptotic figures at any time points (Kume et al., 2004), although nuclear chromatin margination, one of the ultrastructural characteristics of apoptosis, was detected in hepatocyte primary cultures after SZ-treatment (to be published elsewhere).

Fig. 4 shows the relationship between the changes in the cell cycle related genes expression. P53 activation was induced and the cascade for some related genes such as growth arrest and DNA-damage-inducible 45 (GADD45), and cyclin-dependent kinase inhibitor 1A (Cdkn1a, p21) was observed. GADD45 induces G2/M cell cycle checkpoint and make G2/M arrest (Wang et al., 1999), while Cdkn1a induces G1/S arrest (Cazzalini et al., 2003). Thus the present results indicated an existence of cell cycle arrest. This may be supported by the immunohistochemical analysis, in which the ratio of the proliferating cell nuclear antigen (PCNA) positive hepatocytes was low at 24 and 48 h after the SZ-treatment (Kume et al., 2004).

Most of genes related with the lipid and glucose metabolism were down-regulated. In Fig. 5, a cascade which leads to nuclear receptors PPARs or RXR was shown. Almost all factors were down-regulated, and serum lipids levels seemed to increase via a decrease in the expression of LDL-R or other factors. On the other hand, some fatty acid synthesis-related factors such as stearoyl-CoA desaturase (Ntambi, 1995) were also down-regulated, although these factors act to decrease serum lipids. More over, sterol regulatory element binding factor 1 (Srebf1), which acts in cholesterol synthesis (Wang et al., 1994), was down-regulated, and the downstream factors such as HmgCoA Synthases (Sakakura et al., 2001) were also down-regulated, although the cascade has not figured. These findings

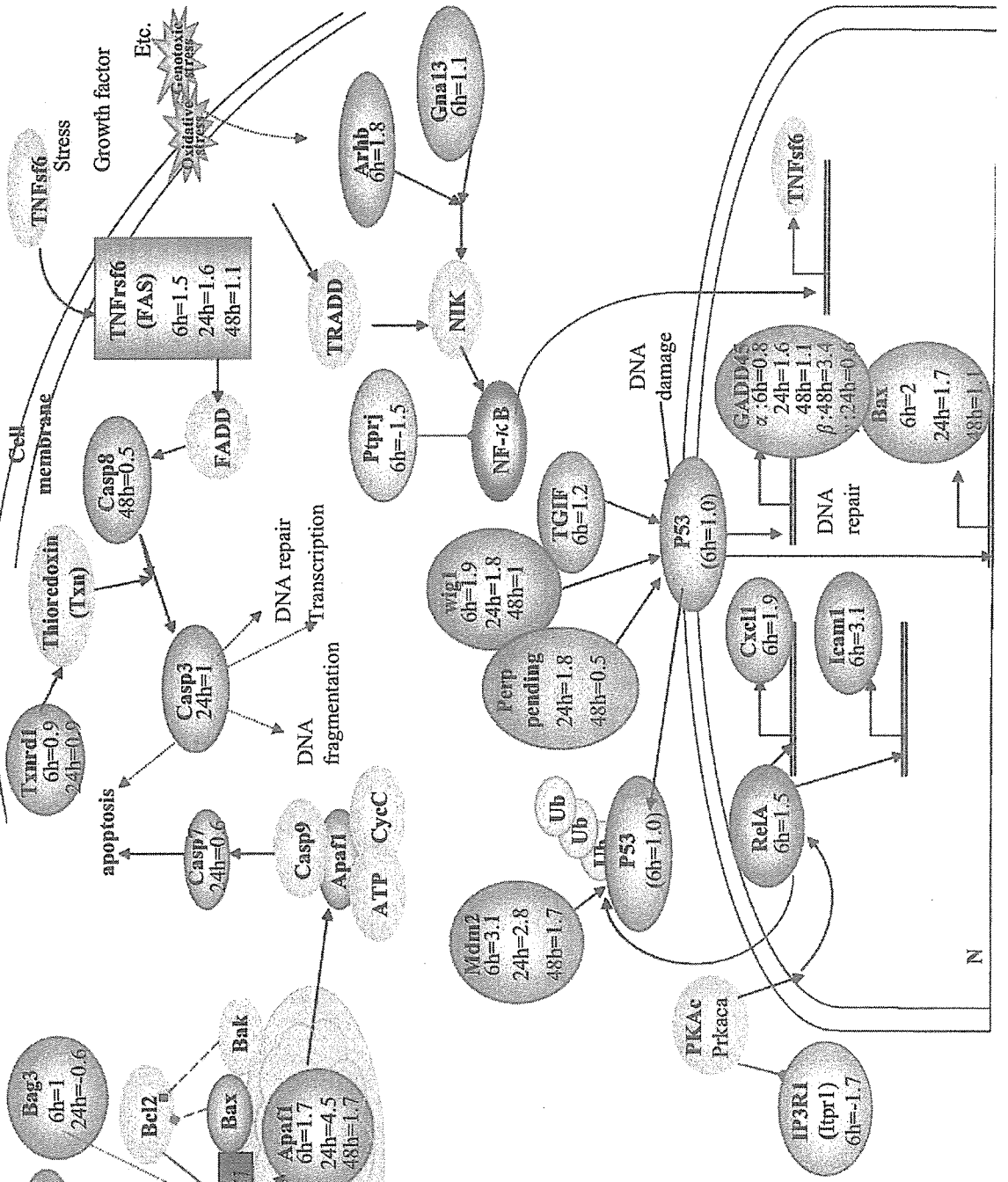

Fig. 3. Hypothetical signal transduction in the liver of the SZ- treated mice (figured by using TransPath program). Numeral represents the SLR of the signal of the probe sets of the SZ-treated mice/the control mice (1): Apoptosis related genes.

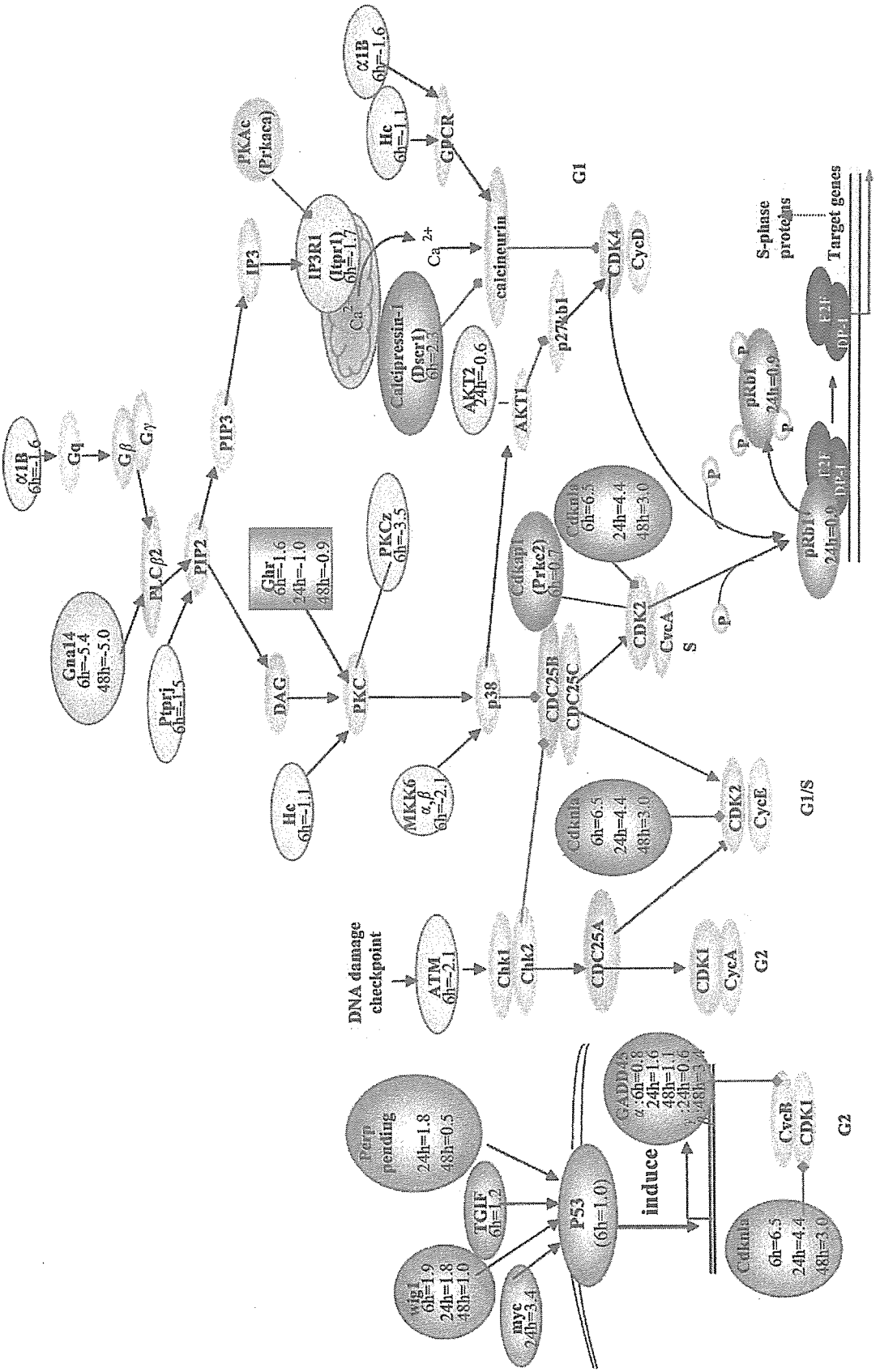

Fig. 4. Hypothetical signal transduction in the liver of the SZ-treated mice (figured by using TransPath program). Numeral represents the SLR of the signal of the probe sets of the SZ-treated mice/the control mice (2): Cell cycle related genes.

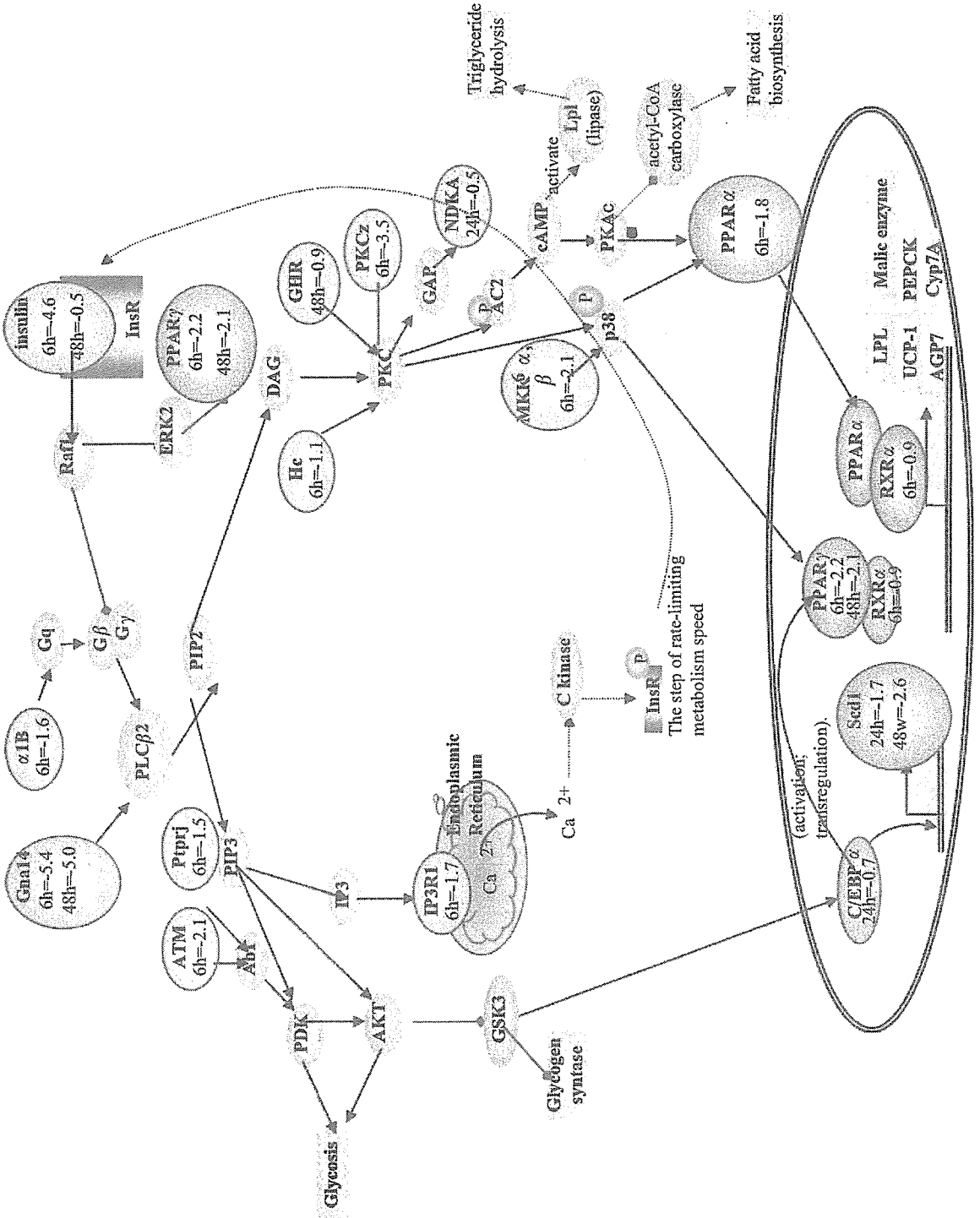

Fig. 5. Hypothetical signal transduction in the liver of the SZ-treated mice (figured by using TransPath program). Numeral represents the SLR of the signal of the probe sets of the SZ-treated mice/the control mice (3): PPAR related genes.

may not indicate that SZ controls these parameters directly, but may indicate that the energy for the lipid and glucose metabolism was not supplied due to the hepatocyte injury.

In conclusion, from the gene expression analysis of the liver of the SZ-treated mice, several changes suggesting the induction of apoptosis, inhibition of cell cycle and decreases in lipid metabolisms were observed. These changes started prior to the elevation of the serum glucose levels, indicating the direct action of SZ on the liver, rather than the secondary effect of diabetes. This may be related with the previously reported hepatic changes such as lipid peroxidation, mitochondrial swelling, and inhibition of hepatocyte proliferation observed before the development of hyperglycemia (Kume et al.. 2004).

Acknowledgment

We thank Mr. S. Kurabe, Ms. M. Kurabe, Ms. E. Ohtsuka, Ms. N. Shimazu, and other members of our laboratory for their technical assistance.

Reference

Cao SX, Dhahbi JM, Mote PL, Spindler SR. Genomic profiling of short- and long-term caloric restriction in the liver of aging mice. Proc Natl Acad Sci USA 2001; 98:10630–5.

Cazzalini O, Perucca P, Riva F, Stivala LA, Bianchi L, Vannini V, Ducommun B, Prosperi E. p21CDKN1A does not interfere with loading of PCNA at DNA replication sites, but inhibits subsequent binding of DNA polymerase delta at the G1/S phase transition. Cell Cycle 2003;2: 596–603.

Cecconi F, Alvarez-Bolado G, Meyer BI, Roth KA, Gruss P. Apaf1 (CED-4 homolog) regulates programmed cell death in mammalian development. Cell 1998;94:727–37.

Dhahbi JM, Mote PL, Cao SX, Spindler SR. Hepatic gene expression profiling of streptozotocin-induced diabetes. Diabetes Technol Ther 2003;5:411–20.

Doi K, Yamanouchi J, Kume E, Yasoshima A. Morphologic changes in hepatocyte nuclei of streptozotocin (SZ)-induced diabetic mice. Exp Toxic Pathol 1997;49:295–9.

Gottlieb TM, Leal JF, Seger R, Taya Y, Oren M. Cross-talk between Akt, p53 and Mdm2: possible implications for the regulation of apoptosis. Oncogene 2002;21:1299–303.

Hellborg F, Qian W, Mendez-Vidal C, Asker C, Kost-Alimova M, Wilhelm M, Imreh S, Wiman KG. Human wig-1, a p53 target gene that encodes a growth inhibitory zinc finger protein. Oncogene 2001;20:5466–70.

Kaelin Jr WG. The p53 gene family. Oncogene 1999;18: 7701–5.

Kume E, Doi C, Itagaki S, Nagashima Y, Doi K. Glomerular lesions in unilateral nephrectomized and diabetic (UN-D) mice. J Vet Med Sci 1992;54:1085–90.

Kume E, Itagaki S, Doi K. Cytomegalic hepatocytes and bile duct hyperplasia in streptozotocin-induced diabetic mice. J Toxicol Pathol 1994a;7:261–5.

Kume E, Ohmachi Y, Itagaki S, Tamura K, Doi K. Hepatic changes of mice in the subacute phase of streptozotocin (SZ)-induced diabetes. Exp Toxic Pathol 1994b;46:368–74.

Kume E, Fujimura H, Matsuki N, Ito M, Aruga C, Toriumi W, Kitamura K, Doi K. Hepatic changes in the acute phase of streptozotocin (SZ)-induced diabetes in mice. Exp Toxic Pathol 2004;55:467–80.

LeBlanc H, Lawrence D, Varfolomeev E, Totpal K, Morlan J, Schow P, Fong S, Schwall R, Sinicropi D, Ashkenazi A. Tumor-cell resistance to death receptor–induced apoptosis through mutational inactivation of the proapoptotic Bcl-2 homolog Bax. Nat Med 2002;8:274–81.

Lee JH, Takahashi T, Yasuhara N, Inazawa J, Kamada S, Tsujimoto Y. Bis, a Bcl-2-binding protein that synergizes with Bcl-2 in preventing cell death. Oncogene 1999;18: 6183–90.

Ntambi JM. The regulation of stearoyl-CoA desaturase (SCD). Prog Lipid Res 1995;34:139–50.

O'Connor L, Strasser A, O'Reilly LA, Hausmann G, Adams JM, Cory S, Huang DC. Bim: a novel member of the Bcl-2 family that promotes apoptosis. EMBO J 1998;17:384–95.

Robles AI, Bemmels NA, Foraker AB, Harris CC. APAF-1 is a transcriptional target of p53 in DNA damage-induced apoptosis. Cancer Res 2001;61:6660–4.

Sakakura Y, Shimano H, Sone H, Takahashi A, Inoue N, Toyoshima H, Suzuki S, Yamada N, Inoue K. Sterol regulatory element-binding proteins induce an entire pathway of cholesterol synthesis. Biochem Biophys Res Commun 2001;286:176–83.

Schott AF, Apel IJ, Nunez G, Clarke MF. Bcl-XL protects cancer cells from p53-mediated apoptosis. Oncogene 1995;11:1389–94.

Sibay TM, et al. The study and effect of streptozotocin (NSC-37917) rendered diabetic chinese hamsters. Ann Ophthalmol 1971;3:596–601.

Steffes MW, Mauer SM. Diabetic glomerulopathy in man and experimental animal models. Int Rev Exp Pathol 1984;26: 147–75.

Susztak K, Bottinger E, Novetsky A, Liang D, Zhu Y, Ciccone E, Wu D, Dunn S, McCue P, Sharma K. Molecular profiling of diabetic mouse kidney reveals novel genes linked to glomerular disease. Diabetes 2004;53:784–94.

Vavra JJ, DeBoer C, Dietz A, Hanka LJ, Sokolski WT. Streptozotocin, a new antibacterial antibiotic. Antibiotics Anual 1960; 230–235.

Wada F, et al. Gene expression profile in streptozotocin-induced diabetic mice kidneys undergoing glomerulosclerosis. Kidney Int 2001;59:1363–73.

Wang X, Sato R, Brown MS, Hua X, Goldstein JL. SREBP-1, a membrane-bound transcription factor released by sterol-regulated proteolysis. Cell 1994;77:53–62.

Wang XW, Zhan Q, Coursen JD, Khan MA, Kontny HU, Yu L, Hollander MC, O'Connor PM, Fornace Jr AJ, Harris CC. GADD45 induction of a G2/M cell cycle checkpoint. Proc Natl Acad Sci USA 1999;96:3706–11.

White FR. Streptozotocin. Cancer Chemother Rep 1963;30: 49–53.

Available online at www.sciencedirect.com
SCIENCE DIRECT®
ELSEVIER
Experimental and Toxicologic Pathology 56 (2005) 245–253
EXPERIMENTAL AND TOXICOLOGIC PATHOLOGY
www.elsevier.de etp

Morphological and gene expression analysis in mouse primary cultured hepatocytes exposed to streptozotocin

Eisuke Kume[a,*], Chinami Aruga[a], Kaori Takahashi[a], Satoko Miwa[a], Eriha Dekura[a], Masahito Itoh[a], Yukiko Ishizuka, Hisako Fujimura[a], Wataru Toriumi[a], Kunio Doi[b]

[a]*Exploratory Toxicology and DMPK Research Laboratory, Tanabe Seiyaku Co. Ltd., 2-2-50, Kawagishi, Toda, Saitama 335, Japan*
[b]*Department of Veterinary Pathology, Graduate School of Agricultural and Life Sciences, The University of Tokyo, Tokyo, Japan*

Received 9 September 2004; received in revised form 28 October 2004; accepted 2 November 2004

Abstract

Streptozotocin (SZ) is known to exert toxic effects not only on pancreatic islet beta cells but also on other organs including the liver. For analyzing direct effects of SZ on hepatocytes, we performed morphological analysis and DNA microarray analysis on mouse primary cultured hepatocytes. Hepatocytes were taken from non-treated Crj:CD-1(ICR) mice. The primary cultured hepatocytes were treated with SZ at concentrations of 0, 1, 3, 10, 30 and 100 mM. After the treatment for about 6 or 24 h, cell survival assay using tetrazolium salt (WST-1), light microscopic/electron microscopic analysis and gene expression analysis were performed. For the gene expression analysis, target (labeled cRNA) prepared from total RNA of the hepatocytes was hybridized to the GeneChip Murine Genome U74A V.2 (Affymetrix). The signal intensity calculation and scaling were performed using Microarray Suite Software Ver 5.0. IC50 of the cell survival assay was around 62 mM at 6 h exposure and 7 mM at 24 h exposure. Marked chromatin margination was observed in nuclei of the hepatocytes treated with SZ at concentrations of 3 or 10 mM. Gene expression analysis revealed similar expression changes to those of in vivo, i.e. up-regulation in cell proliferation/apoptosis related genes, and down-regulation of lipid metabolism related genes. These results potently supported the hypothesis that many of the hepatic alteration including histopathological and gene expression changes are induced by direct effect of SZ rather than by the secondary effect of the hyperglycemia or hypoinsulinemia.

Keywords: Streptozotocin; In vitro; Hepatocyte; Apoptosis; Gene expression; DNA microarray; Mouse

Introduction

Streptozotocin (SZ) has been attracting a great attention as a useful tool for the induction of diabetes mellitus and its complications in laboratory rodents (Sibay et al., 1971; Steffes and Mauer, 1984; Kume et al., 1992) because of its toxic action on islet β cells. However, SZ is known to exert toxic effects not only on pancreatic islet β cells but also on other organs including liver.

We have previously reported the details of SZ-induced hepatic lesions in the acute (6–48 h after the treatment) and the subacute (4–12 weeks after the treatment) phase (Kume et al., 1994a, b; Doi et al., 1997; Kume et al.,

*Corresponding author. Tel.: +81 48 433 8122; fax: +81 48 433 8171.
E-mail address: e-kume@tanabe.co.jp (E. Kume).

0940-2993/$ - see front matter © 2004 Elsevier GmbH. All rights reserved.
doi:10.1016/j.etp.2004.11.001

2004). Those studies characterized the pathological changes such as the appearance of oncocytic hepatocytes, cytomegalic hepatocytes and bile duct hyperplasia in the subacute phase. In the acute phase, SZ induced several hepatic changes including lipid peroxidation, mitochondrial swelling, peroxisome proliferation and inhibition of hepatocyte proliferation before the elevation of the serum glucose levels (Kume et al., 2004). We also analyzed molecular genetic changes in the liver before and after the induction of hyperglycemia using the Affymetrix GeneChip. Many of the up-regulated genes were categorized into cell cycle/apoptosis-related genes, immune/allergy-related genes and stress response/xenobiotic metabolism-related genes. On the other hand, genes related to glucose, lipid and protein metabolisms were down-regulated (Kume et al., in press). These morphological and genetic changes occurred before the induction of hyperglycemia. Therefore, it is suggested that those changes were attributable to the direct effects of SZ on hepatocytes rather than the secondary effects of diabetes or hyperglycemia.

Several reports have focused on the toxic mechanisms of SZ in islet cells in vitro (Ledoux and Wilson, 1984; Flament and Remacle, 1987; Eizirik et al., 1993; Turk et al., 1993; Bellmann et al., 1995), however, no researchers reported detailed changes in SZ-treated hepatocytes in vitro. Morphological examinations and gene expression analysis were performed on the SZ-treated mouse primary hepatocytes to clarify direct effects of SZ on hepatocytes.

Materials and methods

The study was approved by the Ethical Committee at Tanabe Seiyaku Co. Ltd., and all efforts were made to minimize animal suffering.

Animals

Two 8-week-old male Crj:CD-1(ICR) mice (Charles River Japan Inc., Kanagawa, Japan) were used.

Primary cultured hepatocytes

Hepatocytes were isolated from the mice with use of collagenase perfusion under pentobarbital anesthesia. The isolated hepatocytes were seeded at a density of 1.0×10^6 cells per 35 mm dish in 2 mL medium (William's E medium containing 5% FCS, 0.1 μM dexamethasone, 6.25 μg/mL insulin, 6.25 ng/mL transferrin, 6.25 ng/mL selenium, 100 U/mL penicillin, 100 μg/mL streptomycin, and 50 μg/mL Matrigel). At 24 h after seeding, SZ was applied on the hepatocytes within the same medium for 6 or 24 h at 37 °C. Applied concentrations were selected as 0, 1, 3, 10, 30 and 100 mM. In all 4, 2, and 2 dishes of each concentration were provided for an analysis of cell survival rate, electron microscopic examination, and GeneChip analysis, respectively. Phase contrast micrographs were taken from the dishes for electron microscopic examination.

Cell survival rate (WST-1 assay)

After the 6 or 24 h-incubation with SZ, WST-1 (Wako Pure Chemical Industries Ltd., Osaka, Japan) was added for each dish at a final concentration of 15%, and the dish was incubated for another 3 h. Following the incubation, absorbance was read at a wavelength of 450 nm using a spectrophotometer (Bio-Rad Laboratories Inc., CA, USA). Percentage of survival cell was calculated using the following formula: (absorbance of treated dish/absorbance of control dish) × 100. For the calculation of the 50% inhibition concentration (IC50) value, concentration-response data were fit by non-regression analysis to sigmoid curves by using the GraphPad Prism program (GraphPad Software Inc., CA, USA).

Morphological examination

After the phase contrast micrographs were taken, hepatocytes were fixed with 2.5% glutaraldehyde and 2.0% formaldehyde, postfixed with 1% osmium tetroxide, and embedded in epoxy resin. Semithin sections were stained with toluidine blue and observed under a light microscope. Ultrathin sections were doubly stained with uranyl acetate and lead citrate and observed under a JEOL-1210 electron microscope (JEOL Co. LTD., Tokyo, Japan).

RNA extraction

Total RNA was isolated as the manual of QIAGEN RNEASY kit (QIAGEN, CA, USA). For lysis of cells and tissues before RNA isolation, Buffer RLT with β-mercaptoethanol was added and incubated for 10 min at 37 °C. Total RNA was extracted by using QIAshredder spin column and RNeasy mini spin column. Absorbance rate of the sample at 260 nm/280 nm was determined.

Affymetrix GeneChip analysis

Total RNA was labeled as described in the GeneChip Expression Analysis Technical Manual (Affymetrix, CA, USA). mRNA was reverse-transcribed into cDNA using SuperScript Choice system (Invitrogen, Tokyo, Japan) and T7-(dT)24 primer (Amersham Biosciences, NJ, USA). The cDNA was converted to labeled cRNA using Bioarray HighYield RNA Transcript Labeling Kit